Free-Water Correction in Diffusion MRI: A Reliable and Robust Learning Approach

Leon Weninger[1], Simon Koppers[1], Chuh-Hyoun Na[2], Kerstin Juetten[2], and Dorit Merhof[1]

[1] Institute of Imaging & Computer Vision, RWTH Aachen University, Germany, leon.weninger@lfb.rwth-aachen.de

[2] Department of Neurosurgery, University Hospital RWTH Aachen, 52074 Aachen, Germany

Abstract. In clinical settings, diffusion MRI can be used for extracting biomarkers such as fractional anisotropy or for revealing brain connectivity based on fiber tractography. Both are impacted by the free-water partial volume effect that arises at the border of cerebrospinal fluid or in presence of vasogenic edema. Hence, in order to robustly track white matter fibers close to cerebrospinal fluid and in presence of edema, or to extract consistent biomarkers in these cases, the diffusion MRI signal needs to be corrected for partial volume effects.
We present a novel method that reproducibly infers plausible free-water volumes across different diffusion MRI acquisition schemes. Based on simulated data closely following the individual characteristics of each measurement, a neural network is trained on synthetic groundtruth data. According to our evaluation, this methodology produces more consistent and more plausible results than previous approaches.

Keywords: Water correction · Diffusion MRI · Edema · Partial volume effects

1 Introduction

In regions near cerebrospinal fluid (CSF) or in presence of vasogenic edema, the signal obtained by diffusion-weighted MRI (DWI) stems from both, the free-water (FW) as well as the parenchyma. Thus, in order to analyze the parenchyma in free-water contaminated voxels, first the signal stemming from FW and parenchyma needs to be disentangled.

Several algorithms that directly estimate the FW proportion have been published. Free-water elimination DTI [8] uses a two compartment model, in which the diffusivity of one compartment (the FW compartment) is fixed to a predefined isotropic diffusion. The diffusion tensor properties of the other compartment are variable, as well as the volume fraction of both compartments. With at least two different spherical shells, i.e. acquisitions with at least two different non-zero b-values, this model can be fitted to the data. If only one shell is acquired, the same model can be fit using spatial regularization [11]. An

adaption of diffusion kurtosis imaging to include FW elimination has also been presented recently [2]. A first deep-learning based FW elimination technique was presented at MICCAI 2018. Molina-Romero et al. [10] used completely synthetic diffusion data, on which they trained a neural network to estimate the tissue compartment fraction. For the synthetic data generation, water is modeled as a predefined isotropic gaussian diffusion, and the diffusion behavior of tissue is modeled as a random uniform distribution. Based on these two descriptions and a tissue volume fraction, synthetic diffusion weighted signals can be generated, and the FW volume fraction predicted. This technique also works independent of the number of b-value shells and is 55x faster than previous approaches. Further, recent advanced diffusion models (e.g. multi-shell multi-tissue CSD [9], DIAMOND [12]), mostly requiring multi-shell acquisitions, also include an isotropic FW compartment in their models. The presented approaches either rely on multi-shell acquisitions, which are often not available for clinical applications, or, according to our evaluation, seem to produce inconsistent results with unrealistic free-water fractions.

We propose a novel approach, that determines the FW volume fraction using a neural network (NN) trained on data directly generated from individual DWI data. Relying on diffusion measurements from regions with known tissue microstructure, such as the corpus callosum (CC), the brain's ventricular system or cortical gray matter, voxels with known tissue properties can be extracted. From these voxels, a synthetic dataset with up to three random fiber compartments and a groundtruth FW volume fraction can be composed. Hence, such a dataset should closely follow the characteristics of FW contaminated voxels. A similar synthetic data generation technique has been successfully used to predict fiber directions [13]. Finally, a NN trained on this data can be used to correctly infer the FW volume fraction of the whole brain. This paper makes the following contributions:

- Creation of synthetic yet plausible data of FW contaminated diffusion signals
- A fast and accurate method for determining FW compartments in DWI, that can be applied to single shell diffusion data
- Thorough comparison with current methods
- An application to clinical data

2 Image Data

Data from the Human Connectome Project (HCP) [6] is used, which provides high-resolution multi-shell DWI data. Three spherical shells (b=1000, 2000 and 3000 s/mm^2) with 90 gradient directions each were acquired in an isotropic resolution of 1.25mm. From this database, the 100 unrelated subjects release was selected.

As a FW volume fraction groundtruth is not available for human brains, we also rely on a synthetic dataset for evaluation. In this dataset, the same gradient scheme as used in the HCP data was employed. Single-fiber white matter

diffusion is simulated as a prolate diffusion tensor with a major eigenvalue of $1.7 \times 10^{-3}\,\mathrm{mm}^2/\mathrm{s}$ and two perpendicular eigenvalues of $0.3 \times 10^{-3}\,\mathrm{mm}^2/\mathrm{s}$. CSF is modeled as an isotropic diffusion tensor with eigenvalues of $3 \times 10^{-3}\,\mathrm{mm}^2/\mathrm{s}$, and GM as an isotropic diffusion tensor with eigenvalues of $0.5 \times 10^{-3}\,\mathrm{mm}^2/\mathrm{s}$. Using up to three randomly selected and rotated WM fibers, a CSF and/or GM compartment, 1,000,000 voxels for which the water compartment proportion is known were obtained. Finally, Rician noise was added with an SNR of 20.

For DWI data of brain tumor patients, we rely on an in-house database. This database includes DWI-acquisitions (b=1000 $\mathrm{s/mm}^2$ single-shell, 64 gradient directions, isotropic voxel size of 2.4mm) next to T1- and T2-FLAIR images of 28 patients. The diffusion data was corrected for susceptibility induced- and eddy current distortions with the tools "topup" and "Eddy" from FSL [14]. The use of this data was approved by a local ethics committee, and the patients gave written consent.

3 Methods

Data extraction and signal generation From a registered T1-image, typical CSF- and gray matter (GM) voxels are extracted using an eroded Fast segmentation [16] mask. Diffusion tensors are fitted for each b-value shell to these voxels. Using these voxels, the mean diffusion of CSF and the mean diffusion of GM is obtained. These values are then used for the generation of the synthetic training data.

However, a single diffusion tensor is not enough to model the diffusion signal of white matter of the whole brain, as diffusion depends on microstructural parameters. Corresponding to the generation of a single-fiber response function in CSD [15], single-fiber white matter (WM) voxels are extracted from voxels within the corpus callosum with a fractional anisotropy (FA) greater than a predefined threshold (FA > 0.7). In contrast to CSD, we keep all extracted single-fiber WM voxels, and fit prolate diffusion tensors for each voxel and each shell (e.g. three diffusion tensors for a three-shell acquisition such as the HCP diffusion sequence) independently. Thus, a variety of diffusion tensors representing different white matter microstructures is obtained.

By superposition of up to three randomly sampled- and rotated single-fiber compartments as well as a GM and CSF compartment, synthetic diffusion weighted signals can be constructed with:

$$S(\mathbf{b}, g, f_{FW}) = f_{FW} S_{FW}(\mathbf{b}) + (1 - f_{FW}) S_{tissue}(\mathbf{b}, g), \tag{1}$$

where $\mathbf{b}$ designates the b-value, g describes the direction of the diffusion sensitizing gradients, and S_{tissue} is modeled with up to three white matter fiber compartments and a GM compartment:

$$S_{tissue}(\mathbf{b}, g) = f_1 S_{gm}(\mathbf{b}) + \sum_{n=2}^{4} f_n R_n(S_{wm}(\mathbf{b}, g)) \tag{2}$$

with random compartment fractions $0 \leq f_{FW} \leq 1$, $0 \leq f_n$, $f_1 + f_2 + f_3 + f_4 = 1$ and $R_n()$ a random rotation in SO(3).

Finally, the constructed signal is distorted with Rician noise with an SNR of 20. Employing this model, an infinite amount of multi-tissue voxels with a known FW fraction can be generated.

Using our methodology, the only assumptions made about diffusive properties are that diffusion of single-fibers can be described with prolate tensors for a single b-value, and that the diffusion for GM and CSF is isotropic. As the diffusion properties are estimated independently for each shell, b-value dependent effects (e.g. kurtosis) are thus included in the synthetic data.

Note that it is implicitly assumed that the extracted single-fiber WM voxels contain no FW. In [1] and [5], a FW volume fraction of less than 2% is reported for such tissue, i.e., this modeling error is less than 2%.

Neural network training A neural network is trained on the simulated raw diffusion data to predict the FW volume fraction f_{FW}. Different network architectures were tested, and an optimum performance network was achieved with 4 fully connected layers in combination with tanh activation functions. As input, the normalized signal attenuation is used. The size of the input is thus dependent on the acquisition scheme. As an example, 270 non-zero diffusion gradients were acquired in the HCP dataset, compared to 64 in the clinical dataset. The initial layer width is automatically adjusted to this data shape. It is halved for each subsequent layer, and the last layer finally has only one output, which is regressed against the FW volume fraction with an L2-loss. Thus, for the exemplary HCP data, the number of artificial neurons of the fully connected layers in this half-hourglass shape is 270-135-67-33-1.

Training time depends on the number of acquisition shells and the number of generated synthetic diffusion weighted signals. By default, we create 25,000 voxels, split into 80% training and 20% test set, use a batch size of 256 and an Adam optimizer with a learning rate of 0.005. A larger training- and test set of up to 1,000,000 voxels was evaluated, but the obtained accuracy did not improve. On a consumer-grade CPU and an implementation in PyTorch, convergence is achieved after 100 epochs in less than a minute for an HCP 3-shell acquisition.

Inference step The trained neural network can finally be used on the signal attenuation of the whole brain to predict the volume fraction of FW in all voxels. Finally, the predicted FW signal can be subtracted from the original signal. FW contaminated voxels, i.e., voxels at the border between WM and CSF, or voxels including a vasogenic edema in glioblastoma cases, can thus be corrected. Consequently, biomarkers (FA, MD) extracted from these voxels are better comparable to other areas in the same brain or to other subjects.

4 Experiments and Results

4.1 Evaluation on healthy subjects

Since FW contamination of healthy, normal-appearing WM without contact to CSF is marginal, one quality hallmark of a FW correction is that biomarkers remain stable in aforementioned regions. Only with such a property, FW correction algorithms can be used for clinical decision making. In order to obtain normal-appearing WM non-adjacent to CSF or GM, an eroded white matter mask was constructed. On this WM skeleton, the FW proportions (f_{FW}) as well as differences in FA before and after correction were analyzed. Results obtained with our methodology as well as those obtained with FWE-DTI [8], the probably most-used approach, and with the recent neural network based FW correction approach (ANN-Syn) [10], are compared in Table 1 for the 100 subjects in the HCP database. The free-water fraction estimated by multi-shell multi-tissue CSD (MSMT-CSD) is also given as a comparison. Different version of MSMT-CSD were initially analyzed, and a recent version of the algorithm that includes the S0-signal in the fitting process [3] showed the best results and was used for all experiments.

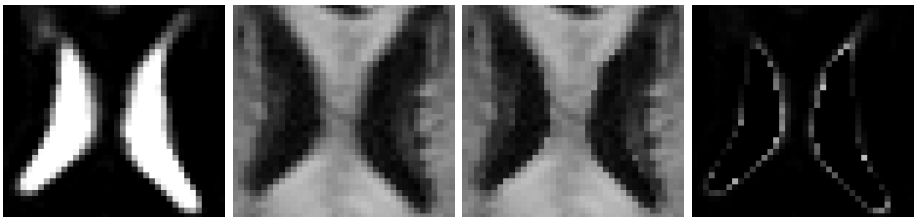

(a) FW-fraction **(b)** FA-map **(c)** After correction **(d)** Difference

Fig. 1: Corpus callosum and lateral ventricles - showcase for FW correction

To further get an impression of b-value dependence, the experiment was replicated for extracted single-shell, two-shell and three-shell data. Implementations were taken from DIPY [4] (FWE-DTI), DMIPY [7] (MSMT-CSD) or from associated Github repositories (ANN-Syn) for all experiments.

Literature states around 1-2% of mean free-water volume fraction in normal-appearing white matter [1, 5]. In order to reliably extract clinically important biomarkers such as FA, free-water correction approaches should not strongly exceed this fraction. Note that FWE-DTI is not applicable to single-shell data, and that diffusion kurtosis effects are not taken into account [8].

In Figure 1, exemplary results of our method on the corpus callosum and lateral ventricles of an HCP subject are shown. Biomarkers (FA, MD) of normal-appearing white matter are not affected by our proposed correction. Meanwhile, the border between CSF and white matter is much sharper – those voxels have been appropriately corrected for the FW compartment.

Table 1: Mean FW volume fraction (f_{FW}) and, where applicable, mean difference between FA before and after FW correction (ΔFA) on WM skeleton. HCP 100 unrelated subjects. Single-shell: b=1000, Two-shell: b=1000 and 2000, Three-shell b=1000, 2000 and 3000 s/mm^2

	Single-shell		Two-shell		Three-shell	
	f_{FW}	ΔFA	f_{FW}	ΔFA	f_{FW}	ΔFA
FWE-DTI	-	-	0.255	0.111	0.309	0.096
ANN-Syn	0.083	0.052	0.196	0.089	0.289	0.097
MSMT-CSD	-	-	0.038	-	0.037	-
Proposed	0.011	0.005	0.011	0.003	0.019	0.004

4.2 Synthetic data analysis

For human brains, a FW volume fraction groundtruth is not available. We thus evaluate the proposed method on the synthetic dataset comprising artificial voxels with multiple compartments.

Table 2: Coefficient of determination (R^2) and mean absolute error (MAE) $\pm$ mean standard deviation of f_{FW} for different water correction approaches on an artificial dataset with SNR=20.

	Single-Shell		Two-Shell		Three-Shell	
	R^2	MAE	R^2	MAE	R^2	MAE
FWE-DTI	/	/	**0.92**	**0.044±0.03**	0.88	0.056±0.03
ANN-Syn	0.89	0.049±0.03	0.85	0.060±0.04	0.06	0.164±0.08
MSMT-CSD	/	/	0.80	0.074±0.03	0.78	0.077±0.03
Proposed	**0.95**	**0.034±0.02**	**0.93**	**0.042±0.02**	**0.93**	**0.040±0.02**

In addition to previous FW correction approaches (FWE-DTI and ANN-Syn), we also analyze the FW compartment predicted by multi-shell multi-tissue CSD. In Table 2, the accuracy of these approaches is compared to our method, by using the coefficient of determination (R^2), the mean absolute error (MAE) and its standard deviation. In all approaches, the corresponding settings for tissue models were selected exactly as for the simulated data. As no segmentation mask is available for this synthetic data, in our model GM- and CSF diffusion properties are also matched to the simulation model, while single-fiber WM is extracted from all voxels with an FA>0.7.

4.3 Application to brain tumor patients

In order to show the clinical relevance of our approach, we applied the presented method on an in-house dataset containing MRI images of 28 brain tumor patients.

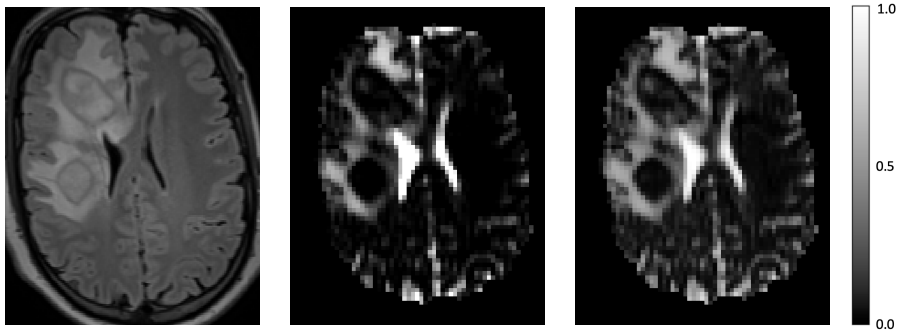

(a) T2-FLAIR image **(b)** Proposed method **(c)** ANN-Syn

Fig. 2: Comparison of the water fraction as estimated by our method compared to the estimation of ANN-Syn, a recent method that is also applicable to single-shell acquisitions. Hyperintensities in the FLAIR image indicate the presence of edema.

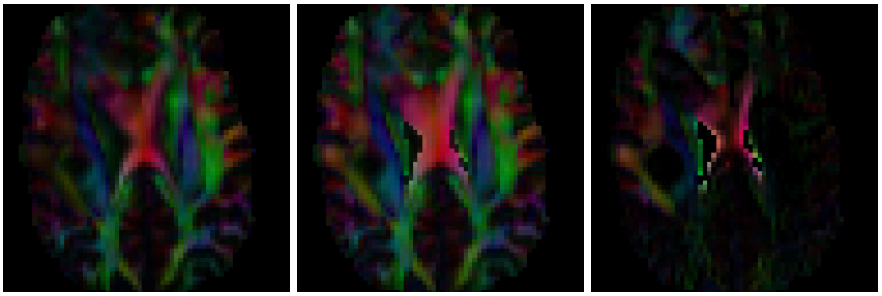

(a) Original FA map **(b)** After correction **(c)** Difference

Fig. 3: Application showcase: Color-FA of a brain tumor patient DWI-acquisition before and after correction.

Figures 2 and 3 show the same patient, highlighting the results of our method. The area affected by edema can be identified as the hyperintense regions in the FLAIR image (Figure 2a). In parts of the brain affected by this edema, the predicted water compartment is between 30% and 40% (Fig. 2b), in accordance

with the FLAIR acquisition. Consequently, after FW correction, these areas now appear brighter in the FA-map (Figure 3), i.e., our method determines the water fraction and exposes the tissue-only signal, thus enabling an improved assessment of this tissue. Further, the border between CSF and WM is much sharper after correction. Meanwhile, normal-appearing white matter, e.g. deep white matter on the contralateral side, is not altered. Compared to ANN-Syn, a recent method that is applicable to single-shell data, the proposed method shows less noise in healthy white matter areas.

5 Discussion

In healthy, normal-appearing WM, our methodology consistently predicts very low FW volume fractions. Here, the estimations of other tested approaches tend to be unreasonably high and fluctuate stronger.

FWE-DTI performs very well on the synthetic dataset, similar to MSMT-CSD. However, it fails for high b-values on the HCP data. This can be explained by the lack of including kurtosis effects, which are present in the real data for high b-values.

In contrast, ANN-Syn fails when including high b-values, both on the HCP data as well as on the synthetic dataset. For the single-shell low b-value case, the results are good. In effect, this method uses random uniform numbers to simulate diffusion data, a pragmatic approach useful for simulation of low b-value diffusion data. However, on the single-shell brain tumor dataset, the free-water estimation in healthy white matter is still noisy.

From the evaluated approaches, our method is the only one that is able to perform free-water correction consistently for different b-value settings. In contrast to FWE-DTI and MSMT-CSD, it takes noise into account, and in contrast to ANN-Syn our employed signal model is more realistic, especially for high b-values.

6 Conclusion

We present a novel, reliable and fast free-water partial volume correction method that is applicable to single- and multi-shell DWI-acquisitions.

Relying on data extracted from the subject, our method is the first that produces coherent and plausible results for different b-values. Subsequent steps, e.g. fiber tracking or biomarker extraction may strongly benefit from this correction, as water-contaminated WM-voxels no longer need to be omitted. Especially in clinical settings with relatively small resolution (e.g. 2.4mm isotropic) such a correction can lead to more robust results.

In patients with brain tumors, our method may allow for a realistic tissue-only biomarker extraction of regions affected by vasogenic edema. Even for healthy subjects, our method supports a more robust extraction of FA values, as voxels at the border between CSF and WM are no longer biased due to free-water partial volume effects.

Acknowledgment Data were provided in part by the Human Connectome Project, WU-Minn Consortium (Principal Investigators: David Van Essen and Kamil Ugurbil; 1U54MH091657) funded by the 16 NIH Institutes and Centers that support the NIH Blueprint for Neuroscience Research; and by the McDonnell Center for Systems Neuroscience at Washington University.

References

1. Bender, B., Klose, U.: Cerebrospinal fluid and interstitial fluid volume measurements in the human brain at 3t with epi. Magnetic Resonance in Medicine **61**(4), 834–841 (2009)
2. Collier, Q., Veraart, J., Jeurissen, B., Vanhevel, F., Pullens, P., Parizel, P.M., den Dekker, A.J., Sijbers, J.: Diffusion kurtosis imaging with free water elimination: A bayesian estimation approach. Magnetic Resonance in Medicine **80**(2), 802–813 (2018)
3. Dhollander, T., Raffelt, D., Connelly, A.: Unsupervised 3-tissue response function estimation from single-shell or multi-shell diffusion mr data without a co-registered t1 image (09 2016)
4. Eleftherios Garyfallidis, Matthew Brett, et al.: Dipy, a library for the analysis of diffusion mri data. Frontiers in Neuroinformatics **8**, 8 (2014)
5. Ernst, T., Kreis, R., Ross, B.: Absolute quantitation of water and metabolites in the human brain. i. compartments and water. Journal of Magnetic Resonance, Series B **102**(1), 1 – 8 (1993)
6. Essen, D.C.V., Smith, S.M., Barch, D.M., Behrens, T.E., Yacoub, E., Ugurbil, K.: The wu-minn human connectome project: An overview. NeuroImage **80**, 62 – 79 (2013), mapping the Connectome
7. Fick, R.H., Wassermann, D., Deriche, R.: Mipy: An Open-Source Framework to improve reproducibility in Brain Microstructure Imaging. In: OHBM 2018 - Human Brain Mapping . pp. 1–4. Singapore, Singapore (Jun 2018)
8. Hoy, A.R., Koay, C.G., Kecskemeti, S.R., Alexander, A.L.: Optimization of a free water elimination two-compartment model for diffusion tensor imaging. NeuroImage **103**, 323 – 333 (2014)
9. Jeurissen, B., Tournier, J.D., Dhollander, T., Connelly, A., Sijbers, J.: Multi-tissue constrained spherical deconvolution for improved analysis of multi-shell diffusion mri data. NeuroImage **103**, 411 – 426 (2014)
10. Molina-Romero, M., Wiestler, B., Gómez, P., Menzel, M.I., Menze, B.H.: Deep learning with synthetic diffusion mri data for free-water elimination in glioblastoma cases. MICCAI (2018)
11. Pasternak, O., Sochen, N., Gur, Y., Intrator, N., Assaf, Y.: Free water elimination and mapping from diffusion mri. Magnetic Resonance in Medicine **62**(3), 717–730 (2009)
12. Scherrer, B., Schwartzman, A., Taquet, M., Sahin, M., Prabhu, S.P., Warfield, S.K.: Characterizing brain tissue by assessment of the distribution of anisotropic microstructural environments in diffusion-compartment imaging (diamond). Magnetic Resonance in Medicine **76**(3), 963–977 (2016)
13. Schultz, T.: Learning a reliable estimate of the number of fiber directions in diffusion mri. In: Medical Image Computing and Computer-Assisted Intervention – MICCAI 2012. pp. 493–500 (2012)

14. Smith, S.M., Jenkinson, M., Woolrich, M.W., Beckmann, C.F., Behrens, T.E., Johansen-Berg, H., Bannister, P.R., Luca, M.D., Drobnjak, I., Flitney, D.E., Niazy, R.K., Saunders, J., Vickers, J., Zhang, Y., Stefano, N.D., Brady, J.M., Matthews, P.M.: Advances in functional and structural mr image analysis and implementation as fsl. NeuroImage **23**, S208 – S219 (2004), mathematics in Brain Imaging
15. Tournier, J.D., Calamante, F., Connelly, A.: Robust determination of the fibre orientation distribution in diffusion mri: Non-negativity constrained super-resolved spherical deconvolution. NeuroImage **35**(4), 1459 – 1472 (2007)
16. Zhang, Y., Brady, M., Smith, S.: Segmentation of brain mr images through a hidden markov random field model and the expectation-maximization algorithm. IEEE Trans Med Imag **20(1):45-57** (2001)